ACCSCIENCE PUBLISHING

INNOSC Theranostics and Pharmacological Sciences

ORIGINAL RESEARCH ARTICLE

Drug repurposing approach for identifying Pfmrk inhibitors as potential antimalarial agents: An *in silico* analysis

Abhishek Sahu*, Tanuj Handa, and Debanjan Kundu

School of Biochemical Engineering, Indian Institute of Technology (Banaras Hindu University), Varanasi, Uttar Pradesh, India

Abstract

Malaria represents a major global health concern, primarily due to the emergence of resistance against most currently available antimalarial drugs. This pressing issue necessitates the discovery of novel antimalarial agents to combat the escalating resistance. A cyclin-dependent kinase (CDK)-like protein, Pfmrk, found in *Plasmodium falciparum*, plays a crucial role in regulating cell proliferation and exhibits a 36.28% sequence homology with its human counterpart hCDK7. Pfmrk forms a complex with plasmodial cyclin (Pfcyc-1) and stimulates kinase activity. Pfcyc-1 from *P. falciparum*, with the highest sequence homology to human cyclin (cyclin H), binds and activates Pfmrk in a cyclin-dependent manner. This discovery provides the first indication that cyclin subunits may regulate both human and plasmodial CDKs in a similar fashion. In this study, we conducted molecular docking and simulation analysis to investigate the interaction between Pfmrk and a selection of the FDA-approved drugs retrieved from the ZINC15 database. The top five drugs – Lurasidone, Vorapaxar, Donovex, Alvesco, and Orap – were screened based on their binding energies, with the best-docked scores ranging between −8 kcal/mol and −12 kcal/mol. Further, evaluation through molecular dynamics simulations for 100 nanoseconds revealed that Lurasidone exhibited the highest binding affinity (−105.90 ± 57.72 kJ/mol) followed by Donovex (−92.877 ± 17.872 kJ/mol). They exhibited stable interactions with the amino acid residues located in the active site of Pfmrk. The results of the *in silico* investigation indicate that Lurasidone and Donovex exhibit antimalarial potential and could serve as promising Pfmrk inhibitors. Further, development of new drugs based on these findings warrants subsequent *in vitro* studies.

Keywords: Pfmrk; *Plasmodium falciparum*; Molecular docking; Drug discovery; Molecular dynamics

***Corresponding author:**
Abhishek Sahu
(abhisheksahu.bce20@itbhu.ac.in)

Citation: Sahu A, Handa T, Kundu D, 2024, Drug repurposing approach for identifying Pfmrk inhibitors as potential antimalarial agents: An *in silico* analysis. *INNOSC Theranostics and Pharmacological Sciences*, 7(1): 1313. https://doi.org/10.36922/itps.1313

Received: June 15, 2023

Accepted: September 6, 2023

Published Online: November 2, 2023

Copyright: © 2023 Author(s). This is an Open-Access article distributed under the terms of the Creative Commons Attribution License, permitting distribution, and reproduction in any medium, provided the original work is properly cited.

Publisher's Note: AccScience Publishing remains neutral with regard to jurisdictional claims in published maps and institutional affiliations.

1. Introduction

The term "Malaria" originates from the Italian word "mal-aria," signifying its association with the noxious air prevalent in regions characterized by stagnant, swampy environments. Malaria is primarily transmitted through the bites of female *Anopheles* mosquitoes carrying the infectious *Plasmodium* species, which belong to the eukaryotic unicellular organisms, classified under the Apicomplexa phylum[1]. Several *Plasmodium* species can infect humans, including *Plasmodium falciparum*, *Plasmodium vivax*,

Plasmodium ovale, and *Plasmodium malariae*. Among these, *P. falciparum* is associated with the most severe and potentially fatal cases of malaria. According to the World Health Organization (WHO), a staggering 300 – 500 million malaria cases are reported annually, with the majority of these cases occurring in Africa. High prevalence is also observed in regions such as India, Sri Lanka, Thailand, Indonesia, Vietnam, China, and Cambodia. In addition, malaria claims the lives of more than 2 million individuals each year[2].

The parasite's complex life cycle involves plasmodial cyclin-dependent kinases (CDKs) and cyclin proteins for its persistence in both vertebrate and invertebrate hosts[3]. These proteins play essential roles in the parasite's survival, both extracellularly and intracellularly. Plasmodial CDKs, such as Pfmrk, belong to the Apicomplex, a specific protein kinase subfamily analogous to CDKs. Pfmrk, akin to CDK7, functions as an upstream kinase, facilitating the activation of multiple CDKs during a cell cycle[4]. It is also known as a CDK-activating kinase due to this role. Pfmrk activates Cdkl, Cdk2, Cdk3, Cdk4, and Cdk6 by activating the C-terminal domain (CTD) of RNA polymerase II through its kinase activity, as shown in Figure 1. Pfmrk exhibits dual functionality in the regulation of gene expression and control of the cell cycle, rendering Pfmrk a promising candidate for drug targeting. Plasmodial cyclins, such as Pfcyc-1 from *P. falciparum*, share the highest sequence homology with human cyclin (cyclin H) and are involved in the activation of Pfmrk in a cyclin-dependent manner. Multiple studies have confirmed that the C-terminal domain of RNA polymerase II serves as an endogenous substrate of Pfmrk[5]. While it has been demonstrated that plasmodial CDKs can be inhibited by mammalian CDK inhibitors[6], the existence of CDK inhibitory proteins in *Plasmodium* remains undiscovered. Therefore, Pfmrk holds promise as a drug target in antimalarial drug screening.

In the present study, we have leveraged this foundational knowledge to determine the potential of selected drugs to interact with and potentially inhibit the Pfmrk protein. The extensive molecular docking and simulation study identified two promising candidate drugs. These drugs warrant further investigation in *in vitro* studies, with the aim of their potential addition to drug panels for malaria treatment in the future.

2. Materials and methods

2.1. Sequence homology between Pfmrk and hCDK7

Sequence homology between Pfmrk and hCDK7 was assessed through multiple sequence alignment, employing the Clustal Omega (1.2.4) tool (https://www.ebi.ac.uk/Tools/msa/clustalo/). The Fast Amino Acid Sequence Search Tool (FASTA) sequence of Pfmrk (ID: P90584) and hCDK7 (ID: P50613) was retrieved from the UniProt database (https://www.ebi.ac.uk/Tools/msa/clustalo/). Subsequently, the Clustal Omega tool was used to estimate the sequence identity between Pfmrk and hCDK7, as shown in Figure S1.

2.2. Protein preparation

In the absence of the experimental structure of the target protein Pfmrk, the FASTA sequence of the target enzyme

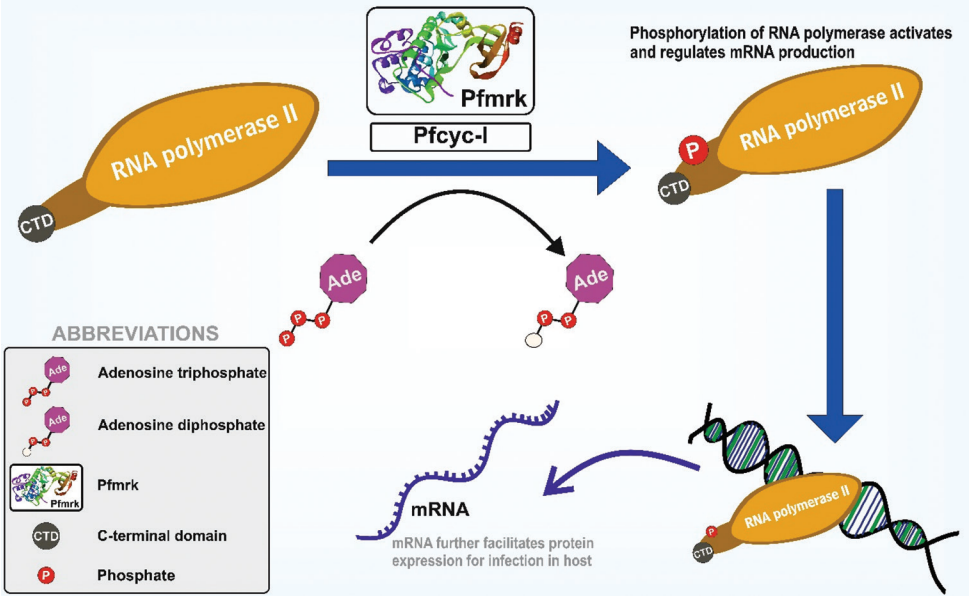


Figure 1. Graphical representation of gene expression induced by Pfmrk through C-terminal domain activation of RNA polymerase II. Pfcyc-1 further activates Pfmrk in a cyclin-dependent manner, with the C-terminal domain of RNA polymerase II serving as a substrate.

Pfmrk (ID: P90584) was retrieved from the UniProt database. To construct the protein model, the Galaxy TBM server[7] was employed, as shown in Figure 2. The model underwent validation using the SAVES v6.0 server PROtein structure CHECKing (PROCHECK)[8] for Ramachandran plot analysis. The model featuring the highest percentage of residues in the most favored region was selected (Figure S2A). In addition, the model's quality was validated using the PROSa webserver (Figure S2B). Subsequently, the modeled protein underwent energy minimization through SWISS Protein Data Bank (PDB) viewer software[9].

2.3. Active site identification and selection for molecular docking

The catalytically active site of Pfmrk comprises specific residues, including L16, M75, M91, I93, and F143, which collectively form a hydrophobic pocket for ATP binding[5]. In hCDK7, the ATP binding site and these five residues differ from those in Pfmrk, featuring distinct amino acids, including D16, I75, F91, F93, and L143 (Waters *et al.*, 2000). To facilitate molecular docking, a grid box was prepared based on these five residues located within the active site of Pfmrk. Detailed information about the amino acids present in the protein's docking site, along with their coordinates, are presented in Table 1.

2.4. Ligand preparation

A total of 1576 compounds available for purchase in the U.S. Food and Drug Administration-approved category were sourced from the ZINC 15 database, provided in MOL2 format (https://zinc.docking.org/substances/subsets/fda+for-sale/). In accordance with Lipinski's rule, these 1576 compounds were screened, and the removal of duplicates, empty structures (salts), isotopes, and inorganic compounds was carried out using the FAF drugs4 server[11]. This process yielded a final database containing 1467 compounds. All compounds from ZINC15 were already in a ready-to-dock conformation. These compounds, provided in MOL2 format, were imported to PyRx software for energy minimization and subsequently converted to the PDB format with charges and atom types (PDBQT) for docking[12].

2.5. Molecular docking and compound screening

Molecular docking was conducted using MGLTools v.1.5.6 Autodock and Raccoon virtual screening tools[13]. The grid was centered on the active site of Pfmrk that contains amino acid residues, and the grid box was constructed with the following coordinate dimensions: center_ x = 266.09, center_y = 319.852, center_z = 310.061, size_x = 60, size_y = 54, size_z = 54. The principal docking protocol incorporated AUTODOCK4 in conjunction with the Lamarckian Genetic Algorithm[13,14]. The compound selection was based on two criteria: the lowest binding free energy (kcal/mol) and the presence of the combination with the highest number of clusters for each compound.

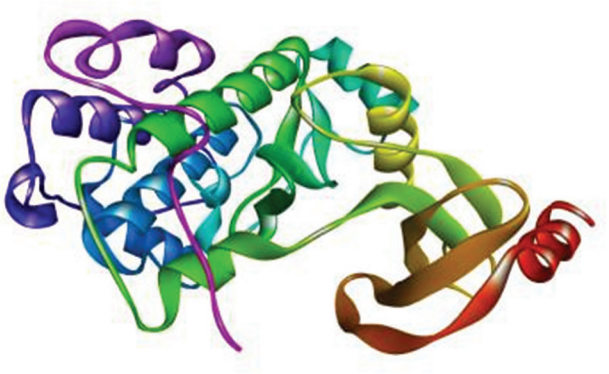


Figure 2. Modeled structure of Pfmrk obtained through Galaxy TBM Web server.

Table 1. Detailed information about the docking proteins, docking sites, and their corresponding coordinates and references

Pfmrk protein sites	Coordinates (X, Y, Z)	Reference
Docking site: Phe15, Lys23, Met91, ILe93, Tyr96, Ser138, Ala140, and Phe143	X_266.09, Y_319.852, Z_ 310.061	[5]
ATP binding site: Leu16, Met75, Met91, Ile93, and Phe143	X_266.09, Y_319.852, Z_310.061	[10]

2.6. Molecular dynamic simulation research

Molecular dynamic simulations were conducted to validate the docking results for Pfmrk and the protein-ligand complexes. Using GROningen MAchine for Chemical Simulations (GROMACS) v 2018.8, the top five drugs were subjected to simulation as a positive control. The PRODRG server version 2.5[15,16] was employed to produce boundary and topographic files for the ligands using the GROMOS force field. The GROMOS 54a7 force field was deployed to prepare both the Pfmrk and ligand complexes. To ensure an appropriate solvation environment, SPC/E water molecules were added to our system, enclosing it within a cubic frame with a dimension of 1.2 nm[17].

During the ionization step, the system was neutralized by adding the appropriate number of Na^+ and Cl^- ions. Energy minimization for all systems was performed with an acceptance of 1000 kJ/mol, and a maximum number of steps was set at 50,000. The particle mesh Ewald (PME) method was deployed to establish a cutoff value of

1.2 nm for both long-range and short-range interactions. In addition, the equilibration procedure for number of particles, volume, and temperature (NVT) and number of particles, pressure, and temperature (NPT) was performed for 1 ns. During this equilibration, the particle number, volume, and temperature were held constant during the post-energy minimization. NVT equilibration was performed using the Berendsen thermostat[15,18] operating with a coupling constant of 0.002 fs at a temperature of 300 K. To identify long-range interactions, the PME method[19] was employed with a cutoff value of 1.2 nm and a Fourier spacing of 0.16 nm. For NPT equilibration, various parameters, including particle count, pressure, and temperature, were fixed. Successful NPT equilibration required the use of the Berendsen isotropic pressure, a time constant of 2 fs, a pressure bar of 1, and isothermal compaction of 4.5×10^{-5} bar. Following the completion of both equilibration steps, simulations for each system were executed for 100 ns with a time step (dt) of 2 fs and a leap-frog integrator[15]. Finally, the simulation results of all the systems were analyzed using standard commands within the GROMACS platform. The LINear Constraint Solver (LINCS) algorithm was used to restrain all bond lengths[14,20].

2.7. Molecular mechanics Poisson-Boltzmann surface area analysis

The molecular mechanics Poisson-Boltzmann surface area (MM-PBSA) method was performed using the gmx_MMPBSA tool and the pbsa.mdp script to evaluate the free binding energy of the top five drugs binding to Pfmrk, along with their respective binding modes. In an effort to optimize computational efficiency, the free energy evaluation was carried out for the final 40 ns of the simulation run. Dielectric constants for both solute and solvent were set at 2 and 80, respectively[14,21,22].

2.8. Visual analysis

The Discovery Studio Visualizer software was used to generate a two-dimensional diagram representing potential interactions within the protein-ligand complex, which serves as a valuable resource for further study (Dassault Systemes BIOVIA 2020). Potential hydrophobic interactions were analyzed using Protein-ligand Interaction Profiler[14].

3. Results

3.1. Docking results

As mentioned earlier, the active site of Pfmrk includes non-conserved amino acids, namely, Phe15, Leu16, Lys23, Met75, Met91, ILe93, Tyr96, Ser138, Ala140, and Phe143. The maximum number of amino acids was enclosed within the grid box. The top five drugs – Lurasidone, Vorapaxar, Donovex, Alvesco, and Orap – exhibited the lowest binding energy and demonstrated the maximum possible interaction with the amino acids situated within the enzyme's active site (Figure 3).

Among these top five drugs, Lurasidone was found to exhibit the lowest binding energy of −12.03 kcal/mol with an inhibitor constant (Ki) of 1.52 nM. Lurasidone forms a non-covalent interaction (alkyl and pi-alkyl) with two critical residues, Ala140 and Phe143, located within the enzyme's Protein Active Site (PAS). Vorapaxar exhibited a binding energy of −10.06 kcal/mol with a Ki of 39.14 nM. Its interaction with the enzyme involves a non-covalent interaction (pi-alkyl) with the essential residue Ile93. Besides these two drugs, Donovex, Alvesco, and Orap exhibited higher binding energy with higher Ki value. These drugs show non-covalent interactions (alkyl and pi-alkyl) with Phe143 and Ala140 key residues within the PAS of the enzyme. Furthermore, a significant non-covalent interaction was observed between Pfmrk and the drug in the ATP-binding region and around our ligand-binding site. A comprehensive overview of these interactions, binding free energy, and Ki, as determined through molecular docking, are shown in Table 2.

3.2. Molecular simulation

The Pfmrk and its associated ligand complexes were simulated for 100 ns, during which five different types of analysis were performed to validate the docking results. To assess the overall stability of the systems, the root-mean-square deviation (RMSD) curve was obtained for both Pfmrk and the holoprotein clusters using the gmx_rms tool. Throughout the simulation, the gmx_gyrate tool was used to calculate the radius of gyration (Rg) of the system. In addition, the root-mean-square fluctuation (RMSF) for the total protein and complex was assessed using the gmx_rmsf tool. To gain insights into the stability of the Pfmrk and complex, the mean number of hydrogen bonds between them was calculated using the gmx_hbond tool. An atomic distance cutoff of 0.35 nm was set between the donors and acceptors.

3.3. RMSD, Rg, and RMSF

The comparison of the RMSD curves between Pfmrk and the other five complexes indicates a close resemblance between the Vorapaxar curve and that of Pfmrk. All five drug complexes exhibited minimal fluctuations, with the curve of all the drugs converging within the range of 0.3 to 0.5 nm. Alvesco and Donovex demonstrated exceptional stability throughout the entire simulation run of 100 ns. The Orap complex exhibited sudden fluctuations up to 40 ns, after which the RMSD remained stable (Figure 4A). In

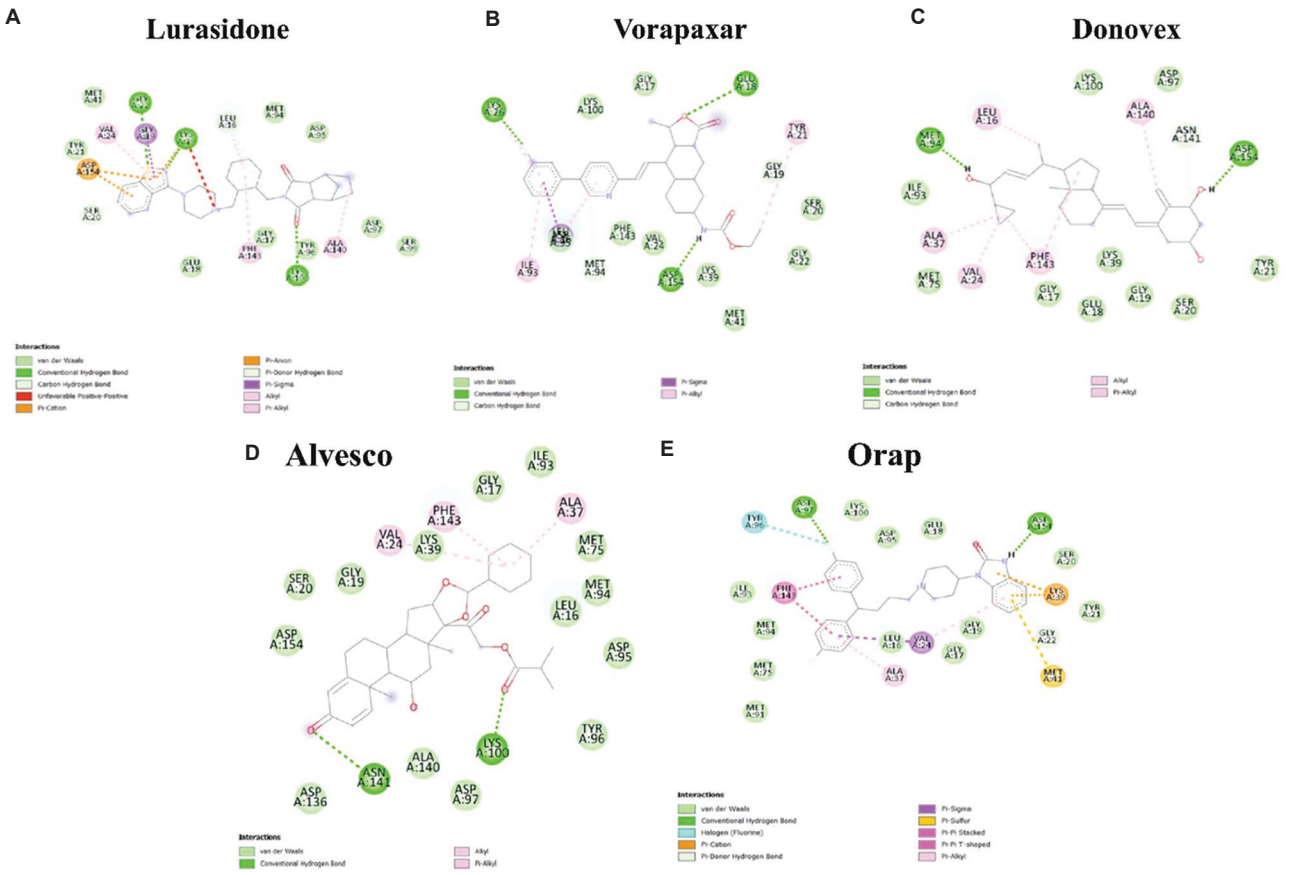


Figure 3. 2D Interaction of Pfmrk with (A) Lurasidone, (B) Vorapaxar, (C) Donovex, (D) Alvesco, and (E) Orap, as visualized in Biovia Discovery studio visualizer.

Table 2. Details of various drugs, their binding energy, Ki values, and interactions with active site residues

FDA-approved drug	Free binding energy (kcal/mol)	Inhibition constant (K_i)	Hydrogen bond interactions	Non-covalent bond interactions
Lurasidone	−12.03	1.52 nM	Lys 39, Lys 100, Gly 22	Leu 16, Val 24, Phe 143 pi-alkyl, Ala 140, Asp 154 (2), lys39 pi-anion, Gly 19 pi-sigma
Vorapaxar	−10.06	39.14 nM	Lys 26, Glu 18, Asp 15,	Ile 93 Pi-alkyl, Tyr 21, Gly 19 C-H bond, Met 94, Leu 16 pi-sigma
Donovex	−8.69	429.05 nM	Met 94 (2), Asp154	Leu 16, Ala 140, Phe 143 (2), Va l24, Ala 37
Alvesco	−8.68	435.75 nM	Asn 141, Lys 100	Val 24 (2), Ala 37, Ala 140, Phe 143
Orap	−8.46	633.3 nM	Asp 154, Asp 97	Lys39 (2), Phe143 (2) Pi-Pi stacked, Ala37 pi alkyl, Met41 Pi cation, Val24, Lys39

terms of Rg, all five complexes displayed a higher degree of compactness compared to Pfmrk. Among them, Donovex, Vorapaxar, and Alvesco exhibited the highest degree of compactness, with the highest deviation of 2.12 nm. Orap and Lurasidone displayed Rg curves resembling that of Pfmrk, which converge at around 2.22 nm (Figure 4B).

According to the docking results, Alvesco and Donovex form a non-covalent interaction with the Ala140, Phe143, and Leu16 residues within the active site of Pfmrk. This interaction results in a reduction of the RMSF curve within the range of residues 15 – 143. Meanwhile, Lurasidone exhibits a superior RMSF curve trajectory within the entire amino acid stretch of 15 – 143 (Figure 5).

3.4. Solvent-accessible surface area (SASA) and hydrogen bonding

The SASA results for all protein-ligand complexes exhibited lower values than Pfmrk, indicating a strong

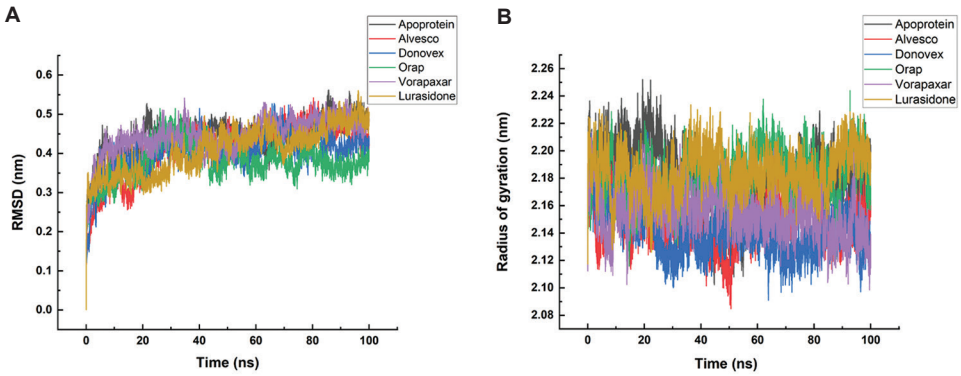


Figure 4. Analysis of the RMSD and Rg results obtained from a molecular dynamics simulation. (A) A comparison of the RMSD trajectories for 100 ns of all protein-ligand complexes and Pfmrks. (B) A comparison of the Rg values for each protein-ligand complex and the Pfmrk over a 100 ns period.

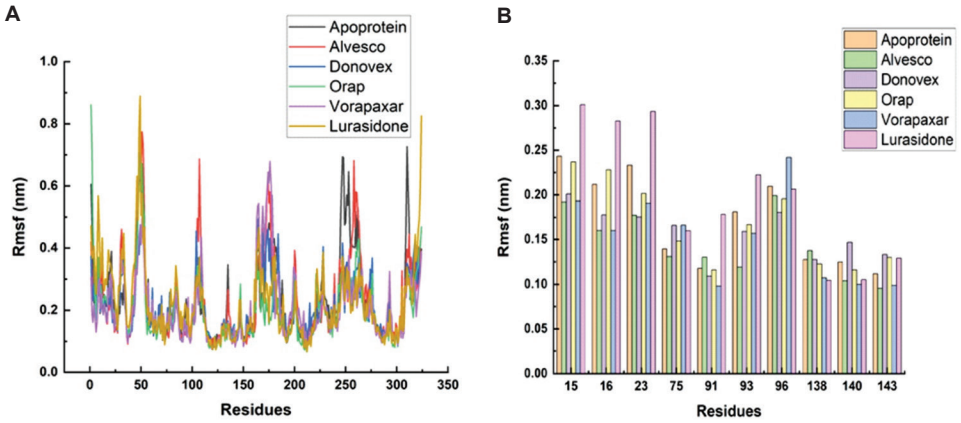


Figure 5. Analysis of the root-mean-square fluctuation (RMSF) results obtained from a molecular dynamics simulation. (A) A comparison of all six drug complexes and the Pfmrk RMSF values for a 100 ns course. (B) A comparison of the RMSF values for the active site residues of each of the six drug complexes and the Pfmrk for a 100 ns course.

binding affinity between the ligands and Pfmrk, consequently increasing the compactness of Pfmrk. These SASA results are presented in Table S1. Simultaneously, the Pfmrk was found to be more folded in the presence of ligands. The Pfmrk complexed with Donovex displayed the lowest SASA value, which contributed to the increased compactness of Pfmrk. The hydrogen bond (H-bond) analysis of all protein-ligand complexes is represented in Table S2. H-bond analysis conducted using MD simulation reveals that Alvesco forms three hydrogen bonds with Lys100, Ser138, and Ala140 and forms an average of one hydrogen bond with the amino acid residues within the active site of Pfmrk.

In contrast, the docking result for Alvesco also reveals the formation of one H-bond (Lys100) under static conditions, as evidenced in our docking results. Donovex forms a more extensive network of hydrogen bonds with amino acids (Met 94, Asp154, Ile 93, Ser138, Ala140, and Phe143). In addition, it forms an average of one H-bond with the residues within the active site of our Pfmrk. Furthermore, the docking result for Donovex forms a two-H-bond (Met 94 and Asp 154). In the case of Lurasidone, it forms hydrogen bonds with specific amino acids (Gly22, Lys39, and Lys100). Furthermore, it forms an average one H-bond with the residues within the active site of our Pfmrk, whereas the docking results for Lurasidone also indicate the formation of a three-H-bond with Gly22, Lys39, and Lys100. Our results indicate that the hydrogen bonds observed during the docking phase often exhibit instability over the course of an extended simulation period. The presence of stable hydrogen bonds is necessary for maintaining stable protein-ligand interactions.

Orap forms two hydrogen bonds with specific amino acids (Lys23 and Asp154) and forms an average of two H-bonds with residues within the active site of our Pfmrk. Conversely, the docking result for Orap indicates the formation of a one-H-bond with Asp154. In comparison, Vorapaxar forms one H-bond with amino acids (Glu18,

Lys26, Tyr96, and Lys100) within the residues of our binding site. This is in contrast to our docking result, which indicated the formation of two H-bonds with Lys 26 and Glu18.

3.5. Secondary structure analysis

The comparative analysis of Dictionary of Protein Secondary Structure (DSSP) secondary structures for both Pfmrk and the ligands was calculated using molecular dynamics simulation and is summarized in Table S3. The secondary structure analysis of Pfmrk reveals similar content in terms of β-sheet, β-bridge, bend, turn, α-helix, 5-helix, and 3-helix when compared to the ligands. In addition, Alvesco and Donovex exhibit a broader range of secondary structures, encompassing coil, β-sheet, β-bridge, and bend. This observation suggests that these ligands have maximum non-covalent interactions with Pfmrk. Orap demonstrates a more significant turn content, signifying its contribution to enhancing protein compactness relative to the other ligands.

3.6. MM-PBSA free energy analysis

The total free binding energy for Donovex was determined to be −92.87 ± 17.87 kJ/mol, while Lurasidone exhibited a slightly higher value of −105.9 ± 57.72 kJ/mol. These energy values were notably higher than those of the other ligands, as indicated in Table 3. Donovex and Lurasidone emerged as the primary contributors to van der Waals forces, underscoring the significance of hydrophobic interactions in our protein-ligand interactions. In addition, these two ligands were observed to exert a notable influence on promoting a more folded state of Pfmrk. Their strong binding affinity was evident through their ability to bind to the protein's active site and other binding regions with relatively higher binding affinity, as reflected in their considerably low binding energy values.

4. Discussion

Malaria remains one of the most dreaded public health concerns, exerting a significant global impact. One of the world's most affected regions by malaria includes certain regions of Africa, where both children and pregnant women are primarily affected. The spread of this deadly disease is influenced by local hygiene and overall environmental conditions. Organizations like the WHO and other leading research institutions continuously strive to improve living conditions and bolster our ability to combat this disease[23-25]. There are two most important strategies for controlling this condition: vector control, which is highly dependent on our living environment, and the development of medicine or vaccines. Although the first vaccine developed for malaria, RTS, S, shows promise, its impact on transmission remains limited, which, in turn, does not significantly affect endemicity[26,27]. The most pressing challenge in managing cases of malaria is the increasing resistance to the current panel of drugs. Drug resistance and cross-resistance among drug combinations are prompting the scientific community to explore alternatives beyond the current array of medications. The review by Pandey *et al*. provides an updated account[23]. As a result, there is an urgent need to identify alternatives, particularly in the most affected regions, including several third-world countries. Therefore, a drug repurposing strategy could be an effective means to screen drugs and expedite the drug development process.

This *in silico* study aims to identify the potential FDA-approved drugs that could target the Pfmrk protein kinase. Through the utilization of molecular docking and subsequent molecular dynamics simulations, we focused on gaining insight into the binding interactions between these screened drugs and Pfmrk's ATP binding site. Our approach particularly focused on the unique characteristics of the active site, marked by the presence of critical residues such as Leu16, Met75, Met91, Ile93, and Phe143. Our findings highlighted the critical role of H-bonds, hydrophobic interactions, and other non-covalent interactions in establishing robust ligand-protein binding.

Given Pfmrk's dual function in both *P. falciparum* cellular replication and its overall life cycle, targeting ATP binding has emerged as a potential strategy to inhibit its kinase activity. Through rigorous analysis, we identified

Table 3. Comprehensive comparative analysis of energetic components in protein-drug complexes formed post-simulation

Ligands	van der Waal energy (kJ/mol)	Electrostatic energy (kJ/mol)	Energy of solvation (kJ/mol)	SASA energy (kJ/mol)	Binding energy (kJ/mol)
Alvesco	−121.789±69.283	−1.518±7.973	65.713±46.072	−13.350±7.725	−70.944±54.776
Donovex	−126.353±20.061	−2.796±2.679	51.327±15.995	−15.054±2.503	−92.877±17.872
Lurasidone	−127.589±64.217	−7.726±7.060	40.816±23.777	−11.408±5.727	−105.907±57.728
Orap	−103.655±100.467	−3.910±6.977	42.897±56.765	−9.701±9.853	−74.369±75.259
Vorapaxar	−5.003±28.557	−0.642±4.782	16.218±40.884	−0.269±4.157	10.304±41.271

Abbreviation: SASA: Solvent-accessible surface area.

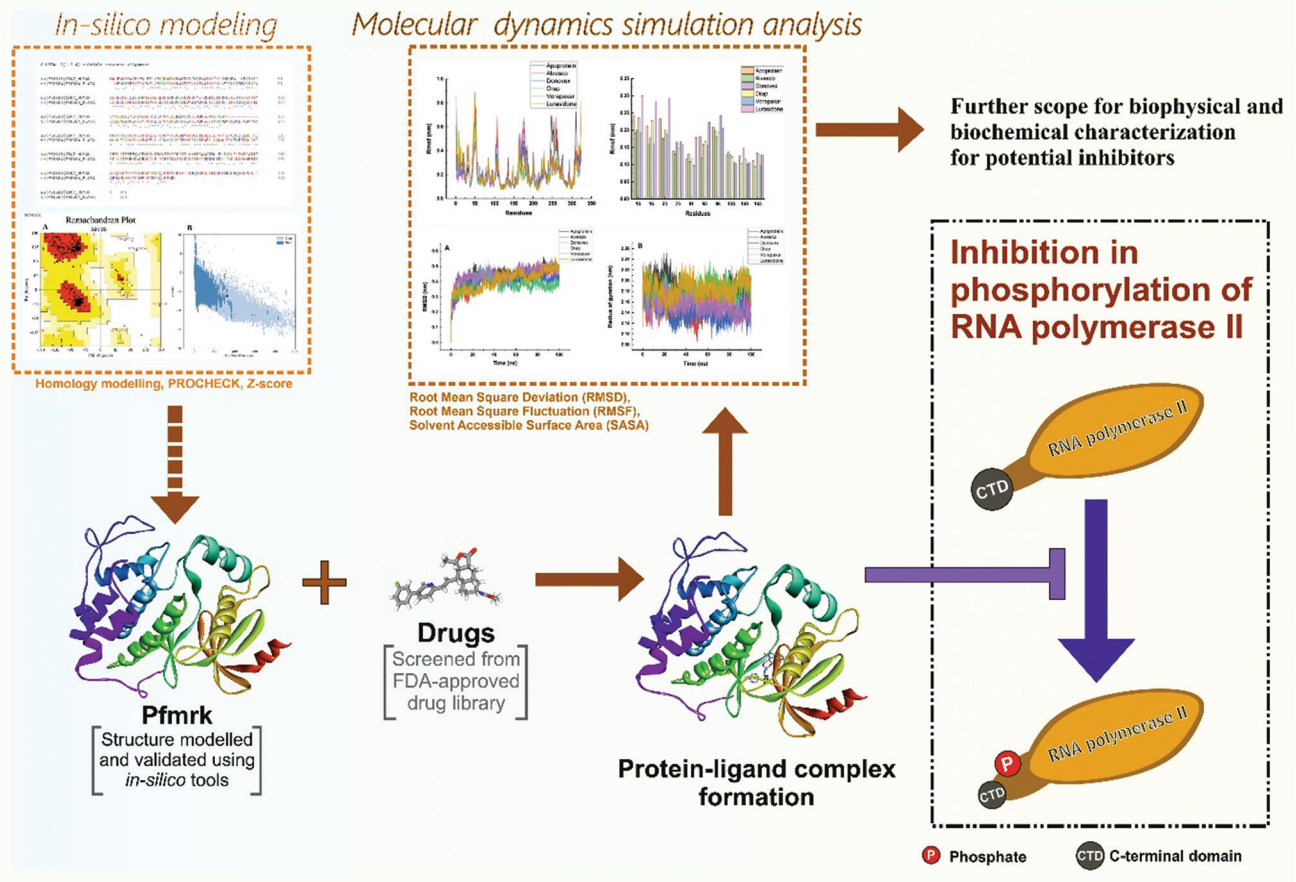


Figure 6. An overview of the entire process involved in this study.

five FDA-approved drugs – Lurasidone, Vorapaxar, Donovex, Alvesco, and Orap – as potential inhibitors due to their strong binding affinities and favorable energy profiles. Furthermore, the original use and year of approval of the FDA-approved drugs is summarized in Table S4. Remarkably, Donovex and Lurasidone yielded the most promising results, characterized by non-covalent interactions with critical residues such as Leu16, Ala140, Phe143, Ile93, and Phe143.

Molecular dynamics simulations provided additional validation for our molecular docking results. These simulations confirmed that Donovex and Lurasidone exhibited strong binding to the ATP binding site, as indicated by our analysis of RMSD, RMSF, Rg, SASA, H-bonding, and MM-PBSA study. These interactions, particularly key residues Ile93 and Phe143, highlighted their potential to inhibit ATP binding, subsequently affecting Pfmrk kinase activity and, ultimately, the transcription machinery.

Significantly, our research addressed the pressing need for new antimalarial targets in light of the growing resistance of *P. falciparum* parasites to existing drugs. Pfmrk has emerged as a promising target, exhibiting a sequence homology of 36.28% with hCDK7. The significant differences between these proteins further highlighted the potential for drug development without harming the host.

5. Conclusion

In this study, we conducted an investigation to explore the potential repurposing of FDA-approved drugs against the Pfmrk protein, a modeled target. Our study identified Alvesco, Donovex, Lurasidone, Orap, and Vorapaxar as potential candidates among FDA-approved drugs, demonstrating strong binding affinities with Pfmrk. Molecular docking and simulation studies further revealed that Donovex and Lurasidone exhibit potential as inhibitors of the modeled Pfmrk protein, acting by binding to its ATP-binding site. The results suggest that Donovex and Lurasidone have the potential to function as kinase inhibitors, making them valuable candidates for further investigation in the context of Pfmrk inhibition. An overview of the entire process involved in this study is illustrated in Figure 6.

In conclusion, our work underlines the significance of targeting Pfmrk as a potential antimalarial strategy. These findings lay a promising foundation for further experimental validation and the development of novel antimalarial drugs.

Acknowledgments

The infrastructure support, the resources and guidance provided by IIT BHU and PARAM Shivay Facility under the National Supercomputing Mission, Government of India at the Indian Institute of Technology BHU, Varanasi are gratefully acknowledged.

Funding

The research supported by research fellowship granted by the Indian Institute of Technology (BHU).

Conflict of interest

The authors declare no conflicts of interest.

Author contributions

Conceptualization: Abhishek Sahu
Formal analysis: Abhishek Sahu, Debanjan Kundu
Investigation: Abhishek Sahu, Tanuj Handa
Methodology: All authors
Writing – original draft: Abhishek Sahu, Debanjan Kundu
Writing – review & editing: All authors

Ethics approval and consent to participate

Not applicable.

Consent for publication

Not applicable.

Availability of data

Data can be requested from corresponding author following formal request.

References

1. Tuteja R, 2007, Malaria- an overview. *FEBS J*, 274: 4670–4679.
2. Breman JG, 2001, The ears of the hippopotamus: manifestations, determinants, and estimates of the malaria burden. *Am J Trop Med Hyg*, 64: 1–11.
   https://doi.org/10.4269/ajtmh.2001.64.1
3. Doerig C, Billker O, Haystead T, *et al*., 2008, Protein kinases of malaria parasites: An update. *Trends Parasitol*, 24: 570–577.
   https://doi.org/10.1016/j.pt.2008.08.007
4. Fisher RP, 2005, Secrets of a double agent: CDK7 in cell-cycle control and transcription. *J Cell Sci*, 118: 5171–5180.
   https://doi.org/10.1242/jcs.02718
5. Keenan SM, Geyer JA, Welsh WJ, *et al*., 2005, Rational inhibitor design and iterative screening in the identification of selective plasmodial cyclin-dependent kinase inhibitors. *Comb Chem High Throughput Screen*, 8: 27–38.
   https://doi.org/10.2174/1386207053328183
6. Li Z, Le RK, Geyer JA, *et al*., 2001, Influence of human p16INK4 and p21CIP1 on the *in vitro* activity of recombinant *Plasmodium falciparum* cyclin-dependent protein kinases. *Biochem Biophys Res Commun*, 288: 1207–1211.
   https://doi.org/10.1006/bbrc.2001.5920
7. Ko J, Park H, Heo L, *et al*., 2012, Galaxy WEB server for protein structure prediction and refinement. *Nucleic Acids Res*, 40: W294–W297.
   https://doi.org/10.1093/nar/gks493
8. Laskowski RA, MacArthur MW, Moss DS, *et al*., 1993, PROCHECK: A program to check the stereochemical quality of protein structures. *J Appl Crystallogr*, 26: 283–291.
   https://doi.org/10.1107/s0021889892009944
9. Guex N, Peitsch MC, 1997, SWISS-MODEL and the Swiss-PdbViewer: An environment for comparative protein modeling. *Electrophoresis*, 18: 2714–2723.
   https://doi.org/10.1002/elps.1150181505
10. Waters PJ, Parniak MA, Akerman BR, *et al*., 2000, Characterization of phenylketonuria missense substitutions, distant from the phenylalanine hydroxylase active site, illustrates a paradigm for mechanism and potential modulation of phenotype. *Mol Genet Metab*, 69: 101–110.
    https://doi.org/10.1006/mgme.2000.2965
11. Lagorce D, Sperandio O, Galons H, *et al*., 2008, FAF-Drugs2: Free ADME/tox filtering tool for drug discovery and chemical biology projects. *BMC Bioinform*, 9: 396.
    https://doi.org/10.1186/1471-2105-9-396
12. Dallakyan S, Olson AJ, 2015, Small molecule library screening by docking with PyRx. *Methods Mol Biol*, 1263: 243–250.
    https://doi.org/10.1007/978-1-4939-2269-7_19
13. Morris GM, Huey R, Lindstrom W, *et al*., 2009, AutoDock4 and AutoDockTools4: Automated docking with selective receptor flexibility. *J Comput Chem*, 30: 2785–2791.
    https://doi.org/10.1002/jcc.21256
14. Kundu D, Dubey VK, 2021, Potential alternatives to current cholinesterase inhibitors: An *in-silico* drug repurposing approach. *Drug Dev Ind Pharm*, 47: 919–930.
    https://doi.org/10.1080/03639045.2021.1952216
15. Borkotoky S, Banerjee M, 2021, A computational

prediction of SARS-CoV-2 structural protein inhibitors from *Azadirachta indica* (Neem). *J Biomol Struct Dyn*, 39: 4111–4121.

https://doi.org/10.1080/07391102.2020.1774419

16. Van Aalten DM, Bywater R, Findlay JB, *et al*., 1996, PRODRG, a program for generating molecular topologies and unique molecular descriptors from coordinates of small molecules. *J Comput Aided Mol Des*, 10: 255–262.

https://doi.org/10.1007/BF00355047

17. Abraham MJ, Murtola T, Schulz R, *et al*., 2015, GROMACS: High-performance molecular simulations through multi-level parallelism from laptops to supercomputers. *SoftwareX*, 1–2: 19–25.

18. Bussi G, Donadio D, Parrinello M, 2007, Canonical sampling through velocity rescaling. *J Chem Phys*, 126: 014101.

https://doi.org/10.1063/1.2408420

19. Kawata M, Nagashima U, 2001, Particle mesh Ewald method for three-dimensional systems with two-dimensional periodicity. *Chem Phys Lett*, 340: 165–172.

20. Hess B, Bekker H, Berendsen HJ, *et al*., 1997, LINCS: A linear constraint solver for molecular simulations. *J Comput Chem*, 18: 1463–1472.

21. Genheden S, Ryde U, 2015, The MM/PBSA and MM/GBSA methods to estimate ligand-binding affinities. *Expert Opin Drug Discov*, 10: 449–461.

https://doi.org/10.1517/17460441.2015.1032936

22. Musyoka TM, Kanzi AM, Lobb KA, *et al*., 2016, Structure-based docking and molecular dynamic studies of plasmodial cysteine proteases against a South African natural compound and its analogs. *Sci Rep*, 6: 23690.

23. Pandey SK, Anand U, Siddiqui WA, *et al*., 2023, Drug development strategies for malaria: With the hope for new antimalarial drug discovery-an update. *Adv Med*, 14: 5060665.

https://doi.org/10.1155/2023/5060665

24. Kelsey A, Stillinger D, Pham TB, *et al*., 2020, Global governing bodies: A pathway for gene drive governance for vector mosquito control. *Am J Trop Med Hyg*, 103: 976–985.

https://doi.org/10.4269/ajtmh.19-0941

25. Nasir SMI, Amarasekara S, Wickremasinghe R, *et al*., 2020, Prevention of reestablishment of malaria: historical perspective and future prospects. *Malar J*, 19: 452.

https://doi.org/10.1186/s12936-020-03527-8

26. Wilson AL, Courtenay O, Kelly-Hope LA, *et al*., 2020, The importance of vector control for the control and elimination of vector-borne diseases. *PLoS Negl Trop Dis*, 14: e0007831.

https://doi.org/10.1371/journal.pntd.0007831

27. Nsanzabana C, 2019, Resistance to artemisinin combination therapies (ACTs): Do not forget the partner drug. *Trop Med Infect Dis*, 4: 26.

https://doi.org/10.3390/tropicalmed4010026